View metadata, citation and similar papers at core.ac.uk

brought to you by CORE

provided by DSpace@MIT

PSFC/JA-07-21

Fast Electron Driven Modes in the Current Rise in Alcator C-Mod.

J.A. Snipes[a], RR. Parker[a], A.E. Schmidt[a], G. Wallace[a] and

P.E. Phillips[b]

December 2007

Plasma Science and Fusion Center
Massachusetts Institute of Technology
Cambridge MA 02139 USA

[a]*M.I.T. Plasma Science and Fusion Center - Cambridge, Massachusetts 02139*

[b]*University of Texas at Austin, Fusion Research Center – Austin, Texas 78712*

This work was supported by the U.S. Department of Energy, Grant No. DE-FC02-99ER54512. Reproduction, translation, publication, use and disposal, in whole or in part, by or for the United States government is permitted.

Submitted for publication to *Physical Review Letters.*

Fast Electron Driven Modes in the Current Rise in Alcator C-Mod

J. A. Snipes, R. R. Parker, A. Schmidt, G. Wallace
MIT Plasma Science and Fusion Center, Cambridge, MA 02139 USA
and
P. E. Phillips
University of Texas at Austin, Fusion Research Center, Austin, TX 78712 USA

The injection of 0.3 – 0.4 MW of Lower Hybrid Current Drive (LHCD) with 90° phasing from the very start of the plasma drives a suprathermal electron tail that excites a series of bursting high frequency (200 – 700 kHz) instabilities in the current rise in Alcator C-Mod. These high frequency bursting modes have relatively small amplitude ($\tilde{B}_\theta \leq 3 \times 10^{-6}$ T) measured with poloidal field pick-up coils on outboard limiters. They are observed very early in the current rise with several bands of frequencies that increase with decreasing density. The frequency at each burst corresponds very closely to the center of the gap frequency for toroidal Alfvén eigenmodes (TAEs), $\omega_{TAE} = v_A / 2qR$, for integer and half integer q values from 11 down to 5.5. Measured average hard x ray photon energies in the range of 25 – 35 keV are in reasonable agreement with the theoretically calculated fast electron energy that matches the precession drift resonance condition for exciting Alfvén eigenmodes.

PACS numbers: 52.35.Bj

Alfvén eigenmodes are excited by energetic ions in almost all tokamaks and stellarators with ion cyclotron radio frequency (ICRF) or neutral beam heating [1-7]. Detailed information on the time evolution of the safety factor (q) in the core is obtained by the frequency evolution of reversed shear Alfvén eigenmodes (RSAEs) or Alfvén cascades in the current rise in tokamaks [8-10]. In addition to the diagnostic use of these modes to determine information about the q profile and the fast ion distribution, understanding how to control them may be very important in future fusion devices such as ITER [11] to control the fusion burn and avoid damage to the first wall. The drive for Alfvén eigenmodes depends on the energy of the particles rather than the mass so that energetic electrons can also drive these modes unstable. Indeed, the precessional drift resonance was first described for fast electrons [12]. Fast electron driven toroidal Alfvén eigenmodes (TAEs) were first seen on Compass-D with combined electron cyclotron heating (ECH) and lower hybrid current drive (LHCD) [13]. Lower frequency fast electron driven fishbone-like bursting modes have also been observed with electron cyclotron current drive (ECCD) on DIII-D [14] and LHCD on FTU [15].

Recent experiments on Alcator C-Mod injecting 300 – 400 kW of LHCD in the current rise drive a suprathermal electron tail that excites high frequency bursting modes unstable. This paper will describe these modes in detail and show how they can be used to determine the evolution of q in the plasma core and provide a measure of the required fast electron energy to drive them unstable that can be compared with hard x ray energy measurements.

Lower hybrid waves are launched into Alcator C-Mod at a frequency of 4.6 GHz with a launcher with 22 operational waveguides toroidally by 4 waveguides poloidally [16]. Current drive phasing of 90° was used in these experiments with corresponding $n_{\|} = 2.3$. The toroidal field was $B_T = 5.4$ T and the plasma current was ramping from 0 up to 0.8 MA. The LH began to couple power just after t=0.02 s and the power coupled well until 0.1 s when the LH was switched off. Suprathermal electrons appear almost as soon as the LH turns on as measured across the radial profile with non-thermal electron cyclotron emission (ECE) measurements [17] as well as with a radially viewing hard x ray camera [18]. The high spatial resolution ECE system has 32 radial channels that span from just inside of the plasma center to the outer edge. The hard x ray camera has 32 channels that span from the top to the bottom of the plasma and can resolve hard x ray photon energies in the range from 20 – 200 keV. High frequency magnetic fluctuations are measured with poloidal field pick-up coils sampled at 2.5 MHz mounted to outboard limiters with up to 10 unequally spaced coils toroidally placed 10 cm above and below the outboard midplane. The closest spaced sets of three coils on each side of the tokamak can measure toroidal mode numbers up to $n < 70$ while several coils spaced farther apart provide low n measurements.

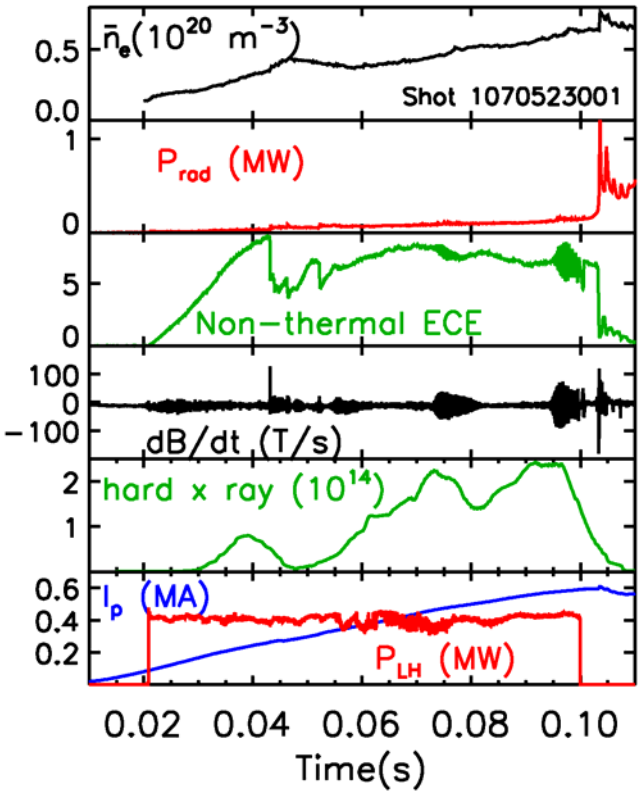

FIG. 1. Time evolution of the line averaged density, total radiated power, non-thermal electron cyclotron emission, poloidal magnetic field fluctuations, hard x ray signal, plasma current, and LHCD power.

Figure 1 gives an overview of a number of plasma parameters as a function of time in the discharge. The LHCD is nearly constant at about 0.4 MW from 0.02 – 0.10 s while the plasma current is ramping from 0 to 0.6 MA. The large hard x ray signal and non-thermal ECE signal clearly show that there is a substantial population of fast electrons present during the LHCD. The electron density is ramping up from near 0 to about $\bar{n}_e \approx 0.6 \times 10^{20}$ m^{-3}. The magnetic fluctuations are dominated by large amplitude ($\tilde{B}_\theta \sim 3 \times 10^{-3}$ T) , low frequency (< 5 kHz) m=2, 3, n=1 oscillations late in the LHCD pulse, which are also visible on the ECE signals. The large amplitude modes lead to a minor disruption just after the LHCD turns off causing a large increase in the total radiated power and a decrease in the plasma current. While these multiple

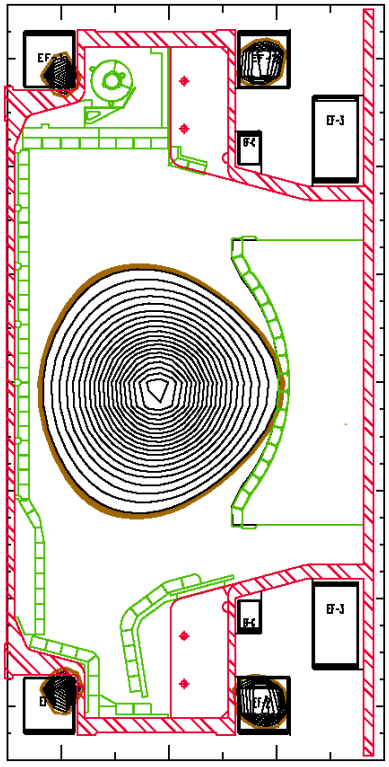

FIG. 2. Poloidal plasma cross-section calculated with EFIT at 0.03 s in the discharge of Fig. 1.

tearing modes are of interest as they indicate that the LHCD is reversing the magnetic shear, this paper will concentrate instead on the small amplitude high frequency modes that appear very early in the LHCD pulse from 0.025 – 0.035 s driven by the fast electrons at high q values.

To determine the plasma shape at these very early times in the discharge, EFIT was run starting at 0.02 s despite the low plasma current, which increases the uncertainty in the quality of the equilibrium reconstruction. Figure 2 shows the poloidal plasma cross-section at 0.03 s indicating that the plasma is outboard limited and nearly fills the vacuum vessel radially. The shape of the last closed flux surface is also used to calculate the line averaged density from the chord length of the central vertical interferometer chord. This density is then used to calculate the expected center of the gap frequency for toroidal Alfvén eigenmodes.

A series of bursting high frequency modes are observed on the magnetic pick-up coils on the outboard limiters just after the start of LHCD in the current rise (Fig. 3a). Three bands of frequencies are observed separated by about 100 kHz. Each burst only lasts about 200 μs, which makes phase analysis of the modes very difficult to accurately determine the mode numbers. A comparison of two successive discharges with different densities shows that the frequency of

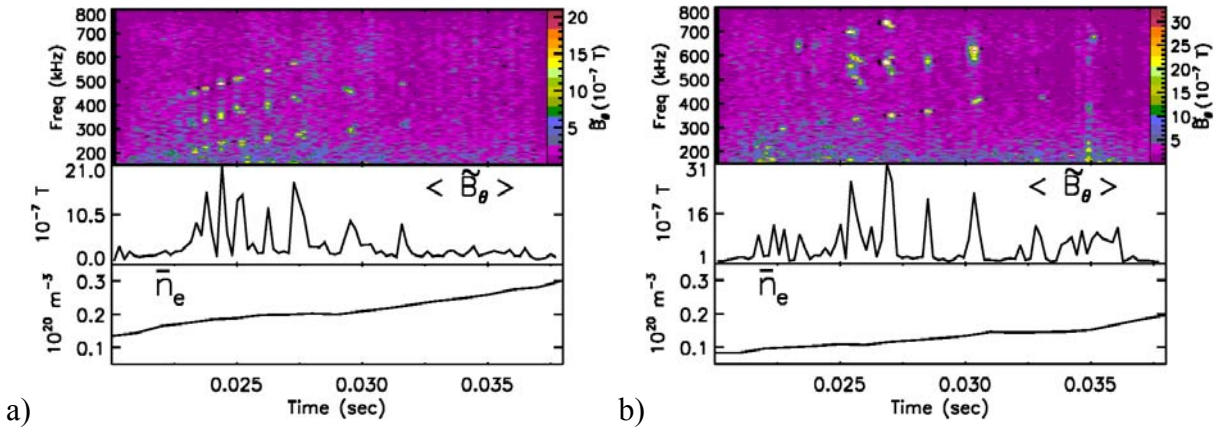

FIG. 3. a) Bursting high frequency modes at higher line averaged density compared with b) lower line averaged density where the mode frequencies and amplitudes are higher. The LHCD power and other plasma conditions were the same for the two discharges.

these bursting modes is higher at lower density, suggesting that the modes may be Alfvén eigenmodes since their frequency is proportional to the Alfvén speed, which goes as $1/\sqrt{n_e}$ (Fig. 3b). The envelope of the mode amplitudes is also shown in Fig. 3, which clearly shows that the amplitude of the modes also increases inversely with density.

Looking closely at the time evolution of these bursting modes, the bursts are observed to be initially very close together in time and then gradually separate more and more as the current rises and the edge q falls. Starting with the lower frequency band of modes, the frequency at each burst can be calculated as a center of the gap TAE frequency given by $\omega_{TAE} = \mathrm{v}_A / 2qR$ using the line averaged density in the Alfvén velocity and the major radius of the magnetic axis. An effective mass of 2.1 was used in the Alfvén velocity for deuterium background ions with an assumed $Z_{eff} = 4.05$, which is not unreasonable during this low density phase of the current rise. In this way, one finds that the q values that best fit the calculated TAE frequency fall nearly exactly on integer and half integer values from q=11 down to q=5.5 for this series of modes (Fig. 4). Not all of the integer and half integer q values appear as bursts and it is not at present clear

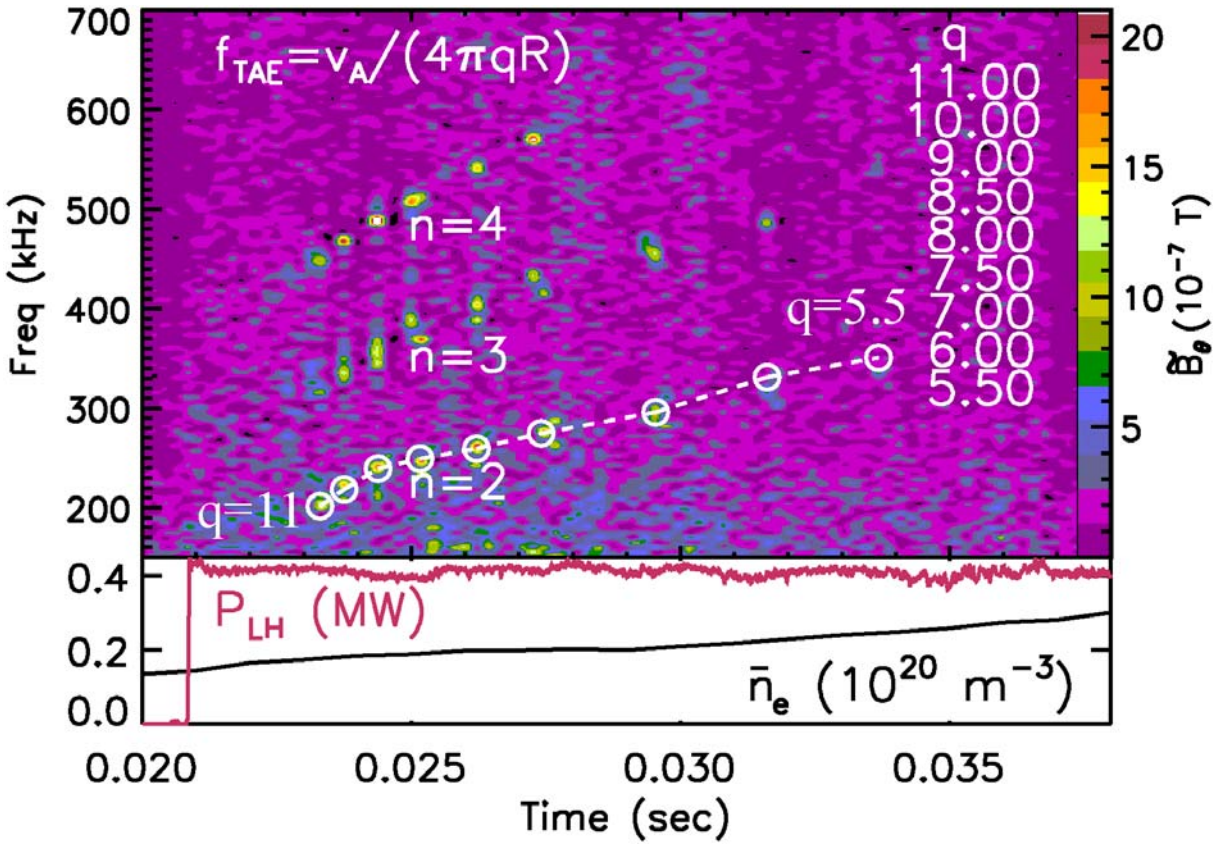

FIG. 4. Bursting high frequency modes from Fig.3 with a fit to the center of the gap TAE frequency overlaid on each burst. The fitted resonant q values fall on integer and half integer values from 11 down to 5.5. The relative frequencies of the three bands of modes scale in approximate proportion as n=2, 3, and 4.

why some values are missing. The two higher frequency bands of modes are approximately at 3/2 and twice the frequencies of the lower frequency band within the width of the TAE gap, indicating that these bands of modes correspond to toroidal modes n=2, 3, and 4. Phase analysis of toroidally separated pick-up coil signals also indicates that the n numbers are in this range, though the very brief bursting nature of the modes makes it difficult to precisely determine the n numbers. Note that there are no clear modes present at lower frequencies where an n=1 mode might be expected. The very precise fit of the measured frequencies to integer and half integer q values indicates that these modes are likely to be TAEs.

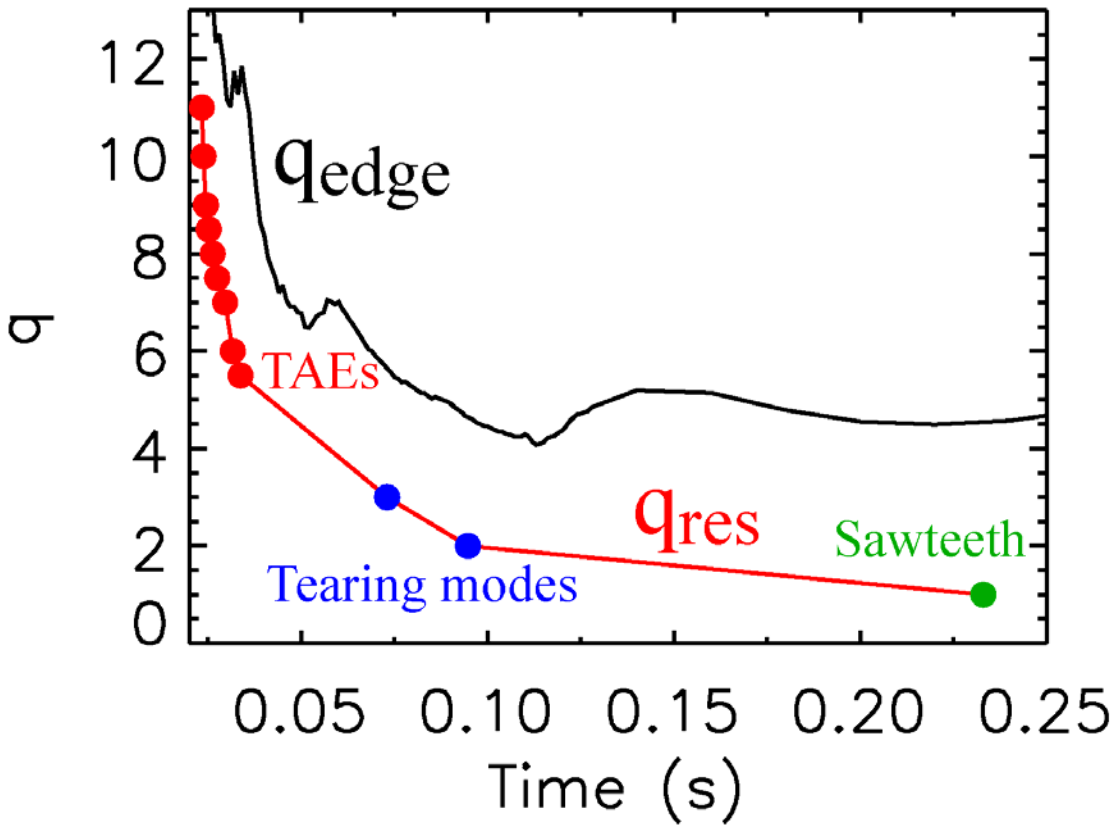

FIG. 5. Time evolution of the EFIT calculated edge q value (black solid line) together with the measured times and resonant q values of the bursting TAEs (red dots), m=3, 2, and n=1 tearing modes (blue dots), and the time of the appearance of sawteeth (green dot).

The evolution of the resonant q values of these bursting modes tracks the time evolution of the edge q value (Fig. 5). In addition to the early TAEs, the time when the large amplitude m=3 and 2, n=1 modes are also shown as well as the time that sawteeth appear in the plasma, which correspond to resonant q values of 3, 2, and 1, respectively. This clearly shows that these resonant q values will be present deep inside the plasma at the time that each mode appears. No further information on the radial location of these high frequency bursting modes is available for these discharges.

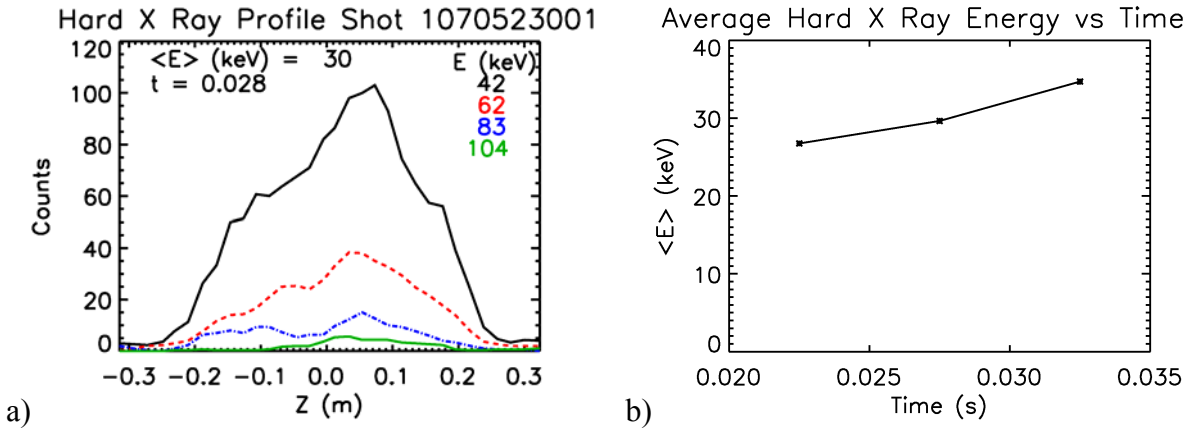

FIG. 6. a) Measured hard x ray line integrated profile for energy bins from 42 to 104 keV at the time of the bursting high frequency modes in Fig. 4. b) Average hard x ray energy across the profile as a function of time during the bursting high frequency modes of Fig. 4.

An important test of whether these high frequency bursting modes are indeed TAEs is whether or not they match a resonance condition for energetic electrons. Figure 6a shows the hard x ray line integrated profiles for energy bins from about 40 keV to just over 100 keV from a radially viewing hard x ray camera. The hard x ray profiles are rather broad with significant counts out to at least 80 keV photon energy. Taking an average of the hard x ray photon counts, Fig. 6b shows that the average hard x ray energy increases from 25 keV to 35 keV during the time that the high frequency bursting modes are observed.

The measurements indicate that there are indeed high energy electrons responsible for the hard x ray emission. Calculations based on similar hard x ray photon energy measurements during LHCD on JET indicate that the fast electron energy is a nonlinear function of the hard x ray photon energy that depends on the anisotropy of the fast electron distribution [19]. Lower hybrid generates an energetic electron tail predominantly in the direction parallel to the magnetic field, but the non-thermal ECE signals (Fig. 1) clearly show that there is also a non-thermal perpendicular component. While the JET calculations are not for precisely the same conditions

as are present in C-Mod during these experiments, these calculations suggest that the fast electron energy is larger than the measured hard x ray photon energy.

A resonant interaction of fast electrons with the precession drift frequency was originally considered to drive fast particle instabilities [12]. Later, 'fishbone' oscillations were explained with the same kind of precession drift instability due to neutral beam ions [20]. More recently, Zonca, et al., have given a simple expression to compare the fast electron energy with the mode frequency for a range of fast particle driven modes to match this resonance condition [15]. Choosing, in the C-Mod case, the expected center of the gap TAE frequency, the expression for the average electron energy that would match the precession drift resonance condition for this mode frequency is approximately $T_h(\mathrm{keV}) \sim 3.07 \times 10^{12} \frac{B^2(\mathrm{T})}{\sqrt{n_i(\mathrm{m}^{-3})}} \frac{r_s(\mathrm{m})}{nq^2}$, where B is the toroidal field on axis, r_s is the minor radius of the mode resonance, n_i is the ion density at the mode resonant surface, n is the toroidal mode number and q is the safety factor of the resonant mode. Taking, B = 5.4 T, $n_i = 2 \times 10^{19}$ m^{-3}, r_s = 0.1 m, n = 2, and q = 5.5 at the highest frequency of the lowest n mode in Fig. 4, $T_h \sim 33$ keV. Given that the mode must be deep inside the plasma compared with the edge q value as shown in Fig. 5, this assumed mid-radius point is not unreasonable. The resulting T_h is very close to the measured hard x ray photon average energy at this time. While there are uncertainties in all of these measurements as well as in the model expression for the resonant fast electron energy, which depends on the anisotropy of the fast electrons, there is quite good agreement between the calculated value of T_h and the measured hard x ray photon energy.

The theoretical dependence of the fast electron energy required to maximize the drive for the precession drift resonance on the toroidal mode number and the resonant q may also explain why the modes disappear early in the discharge despite continued LHCD. As q falls with time, the required fast electron energy to drive the modes increases, so that there may be an insufficient number of fast electrons with high enough energies to drive the modes for $q \leq 5$ and overcome the inherent damping processes. Furthermore, the absence of an unstable n=1 mode may also be because there is an insufficient number of energetic enough fast electrons, since twice the energy would be required for n=1 as for n=2. In this way, the drift precession resonance condition together with the time evolution of these bursting TAEs can be used to constrain the fast electron distribution function.

The authors would like to thank the Alcator C-Mod team, particularly all of the lower hybrid group, for keeping the machine and lower hybrid system running for these experiments. This work was supported by US DoE grant DE-FC02-99ER54512.

[1] King-Lap Wong, Plasma Phys. Cont. Fus. **41,** R1 (1999).
[2] W. W. Heidbrink, *et al.,* Phys. Rev. Lett. **71,** 855 (1993).
[3] A. Fasoli, *et al.,* Plasma Phys. Cont. Fus. **39,** B287 (1997).
[4] M. Saigusa, *et al.,* Plasma Phys. Cont. Fus. **37,** 295 (1995).
[5] J. A. Snipes, *et al.,* Plasma Phys. Cont. Fus. **42,** 381 (2000).
[6] S. Bernabei, *et al.,* Phys. Rev. Lett. **84,** 1212 (2000).
[7] A. Weller, *et al.,* Phys. Rev. Lett. **72,** 1220 (1994).
[8] H. Kimura, *et al.,* Nucl. Fus. **38,** 1303 (1998).
[9] S. Sharapov, *et al.,* Phys. Plasmas **9,** 2027 (2002).
[10] J. A. Snipes, *et al.,* Phys. Plasmas **12,** 056102 (2005).
[11] A. Fasoli, *et al.,* Nucl. Fus. **47,** S264 (2007).
[12] H. P. Furth, Phys. Fluids **8,** 2020 (1965).
[13] M. Valovič, *et al.,* Nucl. Fus. **40,** 1569 (2000).
[14] K. L. Wong, *et al.,* Phys. Rev. Lett. **85,** 996 (2000).
[15] F. Zonca, *et al.,* Nucl. Fus. **47,** 1588 (2007).
[16] P. T. Bonoli, *et al.,* Fusion Science and Technology **51 Number 3,** 401 (2007).
[17] R. Chatterjee, *et al.,* Fusion Engineering and Design **53,** 113 (2001)
[18] J. Liptac, *et al.,* Rev. Sci. Inst. **77,** 103504 (2006).
[19] M. Brusati, *et al.,* Nucl. Fus., **34,** 23 (1994).
[20] Liu Chen, R. B. White, and M. N. Rosenbluth, Phys. Rev. Lett. **52,** 1122 (1984).